

DYNAMICS OF FLEXIBLE RISERS WITH SEABOTTOM UNILATERAL CONTACT

C. A. Almeida

Dept.Mech.Engng, PUC-Rio
calmeida@mec.puc-rio.br

A. T. Andrews

Dept.Mech.Engng, PUC-Rio
atorres@mec.puc-rio.br

Abstract. *This paper deals with an extension of previously published formulation for the dynamic analysis of deepwater line structures such as marine risers, flexible pipelines and offshore loading towers which are, by nature, highly nonlinear. As previously stated, the use of simplified methods such static, quasi-static or frequency domain analysis are powerless techniques when employed to cable dynamics analysis undergoing large displacement motions. In this regard a general, stable and reliable nonlinear finite element representation, applicable to a wide range of underwater line structure analysis, was recently formulated and successfully applied for time domain analysis of underwater cables. The technique, which is based on the separation of rigid body motions and element deformations under finite rotation conditions, considers the position of the cable as defined by a set of co-rotational axes allowing for closed form evaluation of the corresponding finite rotations of the convected coordinate systems. The resulting finite element model incorporates the essential nonlinear effects of the beam element kinematics: coupled axial, bending and torsion deformation measures, element geometry changes, follower forces and pressure effects - all undergoing large displacements, but under small strain assumptions. Generally applied loads to this type of structures such as gravity, buoyancy, wave, current drag and Morison-type loads are all evaluated with respect to the three-dimensional coordinate axes of reference. A specially important feature, when considering the simulation of a riser structure dynamics, is the numerical representation of the cable touching the seabottom. This problem is tackled in the proposed formulation by using special finite element model condition, with Lagrange multipliers. The formulation is, essentially, a displacement based finite element procedure with the introduction of constraint equations through additional unknown interface variables, namely the contact forces. The governing equations were obtained and implemented in a domestic software which gives solutions for the contact region definition, the contact and restraining force vectors and the element displacements and stresses. Prescribed contact conditions considered in the formulation are still restricted to non-slip or to perfect slip conditions. They were solved to demonstrate the applicability of the algorithm to typical cable-bottom interactions, presenting good convergence and accuracy. The numerical results of a sample analysis are evaluated and compared to independent calculations to illustrate the formulation effectiveness in representing the dynamic response of typical underwater line structures.*

Keywords: *cable dynamics, geometric nonlinear effects, unilateral contact, Lagrange multipliers, no-slip and perfect slip friction conditions*

1. Introduction

Due to their very large slenderness, underwater risers are structures possessing low flexural rigidity as compared to the axial rigidity exhibiting large three-dimensional motions under the action of dead, inertia, buoyancy, contact, current and wave loads. This unique characteristic requires the use of numeric nonlinear tools to formulate and to solve for the dynamic response of such slender curvilinear structure members. The problem nonlinearity is further exaggerated as quadratic damping terms - due to fluid drag loads - become present in the resulting discrete system equation of motion. In this case, the solution response is obtained using full Newton-Raphson iterative procedure to accommodate the linearized equation of motion to the solution path, in a step-by-step time integration numerical procedure (Bathe,1996).

In recent years a number of publications have been devoted to the modeling and numerical representation of underwater cable dynamics behavior in the time domain. Basically, they can be classified in three categories: approximations of the cable spatial configuration assuming the slack catenary spatial form, general spatial beam formulations referred to the curvilinear coordinate along the riser centerline, and cable dynamics representation employing classical theory of beams under finite rotations. In the first category, as considered by Ghadimi(1988) and Ractliffe(1984), force equilibrium conditions are directly obtained from the cable spatial configuration, assumed as straight segments. Nodal bending moments are accounted by approximations considering an estimation of the riser curvature from slope changes at the node of two adjoining segments. Inertia is taken into account by lumped masses at the nodes. Although of simple implementation and use, including the seabed-line contact representation, numerical difficulties in the solution convergence have been reported. These occur mainly because inconsistencies on the catenary geometry and the constant beam bending assumptions along adjoining elements, specially in the analysis of cables with

geometries presenting large changes of curvature. In the second, a general finite element approach is considered for the representation of cable dynamics as three-dimension beams, using an updated Lagrangian formulation. This modeling formulation has been carried out by McNamara & Hibbit, 1986 employing the beam-column element formulation with strain measures for axial, torsion, bending and transverse shear. It was stated that in situations where the axial rigidity of a beam is much larger than its bending stiffness, as is the case of a flexible riser, numerical ill-conditioning of the coefficient matrices in the resulting formulation might lead to unstable computations, requiring the introduction of extra constraint equations for inextensibility.

The element formulation used in the present work falls in the third category. As shown in a previous published formulation applied to the dynamics of mooring lines, a three-dimensional finite element scheme related to nonlinear static and dynamics of marine risers and pipelines is considered. The approach consists in the separation of rigid body and deformation kinematics, and the solution of proper coordinate reference frames such that this decomposition is possible. The inherent non-cumulative condition of successive finite rotations about a set of three-dimensional axes is overcome by the use of consistent system of co-rotational axes that are attached to the body of the riser. Therefore, the total rotational displacement at any point along the riser, represented by a transformation matrix, is decomposed into rigid and deformation components. Measures of the rigid body axial rotation are determined by considering the local convective coordinate system, obtained by placing a local axis on the line that supports the element two end nodes with the other two orthogonal axes at the cross-section principal axis of inertia, at one node of the element. Components of the unique transformation tensor \mathbf{T} , representing rotation by an angle α with respect unit vector components p_i , can then be written (Almeida & Lustosa, 1999)

$$T_{ij} = \delta_{ij} - \varepsilon_{ijk} p_k \sin \alpha + p_i p_j (1 - \cos \alpha) \quad (1)$$

where δ_{ij} and ε_{ijk} are, respectively, components of the Kroeneker's delta tensor and the cyclic permutation tensor. This transformation matrix can be decomposed; by using an iterative procedure described in O'Brian et al., 1987 in the following form

$$\mathbf{T} = \mathbf{T}_{def} \mathbf{T}_{rb} \quad (2)$$

where $\mathbf{T}_{rb} = \mathbf{T}_\theta \mathbf{T}_\varphi \mathbf{T}_\psi$ is the transformation matrix from global – initial, undeformed configuration – coordinate axes to local co-rotational system – representing rigid body motions - and \mathbf{T}_{def} is the transformation that incorporates local infinitesimal rotations relative to the co-rotational coordinate axes. The rigid body rotation angles θ , φ and ψ – Euler angles – are directly obtained from vector operations detailed in Lustosa, 2000, with the relative position vector of the element end nodes. Similarly a sequence of operations is performed with \mathbf{T}_{def} (Almeida & Lustosa, 1999) to obtain the element node three rotation angles θ_{def} , φ_{def} and ψ_{def} due to riser deformations. These three angle displacements added to the element centerline relative displacements - u(axial), v and w(transversal) - gives the element total displacement fields which are interpolated by Hermitian functions along the element convective coordinate-x. Therefore, the element axial straining results in

$$\varepsilon_x = u_{,x} + v_{,xx}y + w_{,xx}z + 0.5(u_{,x}^2 + v_{,x}^2 + w_{,x}^2) \quad (3)$$

with the element axial twist and bending curvatures

$$\kappa_x = \psi_{,x} \quad ; \quad \kappa_y = \theta_{,x} \quad ; \quad \kappa_z = \phi_{,x} \quad (4)$$

all needed to obtain the element generalized forces and moments (Almeida & Lustosa, 1999).

The resulting finite element model is a two node Hermitian beam element with, axial, bending and torsion infinitesimal straining expressed with respect to the element degrees-of-freedom, all referred to local (corrotational) coordinate system. The strain-displacement relationship is linear, constrained to infinitesimal Euler beam bending theory and torsion of a straight circular beam, added to second order – quadratic - straining terms, due to cable longitudinal stretching only. From the imposition of the principle of virtual work, equations of motion are derived resulting in a consistent mass matrix and a stiffness matrix which is decomposed in an independent linear and a geometric, element axial stress dependent, non-linear matrix.

In the following the above formulation is extended to incorporate in the cable dynamics contributions of the contact effects with seabed. The study presented is, so far, still restricted to in-plane motion of risers, while in contact with a flat and rigid seabottom, with no friction. Numerical results from the analysis of a “lazy-wave” configuration cable model are presented and discussed, as compared to other published solutions, to illustrate the formulation potential and features in representing the problem, as well as its extension to three-dimension analysis.

$$(\mathbf{n}_j^S)^T [{}^{t+\Delta t}\mathbf{X}_K^{(i)} - {}^{t+\Delta t}\mathbf{X}_P^{(i-1)}] = (\mathbf{n}_j^S)^T [{}^{t+\Delta t}\mathbf{X}_P^{(i)} - {}^{t+\Delta t}\mathbf{X}_P^{(i-1)}]. \quad (6)$$

Using the definitions,

$$\begin{aligned} \Delta \mathbf{u}_P^{(i)} &= {}^{t+\Delta t}\mathbf{X}_P^{(i)} - {}^{t+\Delta t}\mathbf{X}_P^{(i-1)} \\ \text{and} \\ \Delta \mathbf{u}_K^{(i)} &= {}^{t+\Delta t}\mathbf{X}_K^{(i)} - {}^{t+\Delta t}\mathbf{X}_K^{(i-1)} \end{aligned} \quad (7)$$

equation (6) results into the following constraint equation:

$$(\mathbf{n}_j^S)^T [(\Delta \mathbf{u}_K^{(i)} + \Delta_K^{(i-1)}) - \Delta \mathbf{u}_P^{(i)}] = 0 \quad (8)$$

which combined with the second restraint condition

$$(\mathbf{n}_j^S)^T \cdot \Delta \mathbf{u}_P^{(i)} = 0 \quad (9)$$

results in

$$(\mathbf{n}_j^S)^T [\Delta \mathbf{u}_K^{(i)} + {}^{t+\Delta t}\Delta_K^{(i-1)}] = 0, \quad (10)$$

that represents the compatibility restraint condition for the contact under ideal sliding conditions.

For the formulation of the contact solution algorithm, the incremental procedures described in Bathe, 1996 (cap. 6) is used and the above contact condition is imposed by adding to the finite element Variational Indicator the contact forces total potential with constraint of compatible boundary displacements. Therefore, to obtain the equilibrium equations after (i) iterations, at time $t + \Delta t$, we use the following

$$\boldsymbol{\pi}_I^{(i)} = \boldsymbol{\pi}^{(i)} - \sum_K \mathbf{W}_K^{(i)} \quad (11)$$

where $\boldsymbol{\pi}^{(i)}$ is the total potential that furnishes the incremental equilibrium equations at time $t + \Delta t$, after (i) iterations, but with no constraint conditions. $\mathbf{W}_K^{(i)}$ is the total potential of the reaction loads at each node K in the contact region of the cable, after (i) iterations which results, from eq. (10), in

$$\mathbf{W}_K^{(i)} = {}^{t+\Delta t}\lambda_K^{(i)T} [\Delta \mathbf{u}_K^{(i)} + {}^{t+\Delta t}\Delta_K^{(i-1)}] \quad (12)$$

where ${}^{t+\Delta t}\lambda_K^{(i)}$ - Lagrange multiplier coefficient - is the contact force at the riser node K, after (i) iterations.

Variation of the external forces total potential, expressed in equation (12), over all contact nodes and, taking $\delta \Delta_K^{(i-1)} = 0$, results in

$$\delta \sum \mathbf{W}_K^{(i)} = \lambda_K^{(i)} (-\mathbf{n}_j^S)^T \delta \Delta \mathbf{u}_K^{(i)} + \delta \lambda_K^{(i)} (-\mathbf{n}_j^S)^T \Delta \mathbf{u}_K^{(i)} + (-\mathbf{n}_j^S)^T \Delta_K^{(i)} \delta \lambda_K^{(i)} \quad (13)$$

In equation (13) the first two terms represent contributions to the coupling of nodal incremental displacements and contact nodal forces and moments, keeping the system final finite element stiffness matrix symmetric. The third term is a contribution to the forcing vector, associated to the element new degrees-of-freedom. By substituting the results in equation (12) into equation (11) and invoking the stationarity condition $\delta \boldsymbol{\pi}_I^{(i)} = 0$, using the results presented in equation (13), the problem governing equilibrium equations at time $(t + \Delta t)$ are, after $(i-1)$ iterations, in the form

$$\left\{ \begin{bmatrix} {}^{t+\Delta t}\mathbf{K}_C^{(i-1)} & \mathbf{0} \\ \mathbf{0} & \mathbf{0} \end{bmatrix} + \begin{bmatrix} \mathbf{0} & {}^{t+\Delta t}\mathbf{K}_\lambda^{(i-1)} \\ {}^{t+\Delta t}\mathbf{K}_\lambda^{(i-1)T} & \mathbf{0} \end{bmatrix} \right\} \begin{bmatrix} \Delta \mathbf{U}^{(i)} \\ \boldsymbol{\lambda}^{(i)} \end{bmatrix} = \begin{bmatrix} {}^{t+\Delta t}\mathbf{R} \\ \mathbf{0} \end{bmatrix} - \begin{bmatrix} {}^{t+\Delta t}\mathbf{F}^{(i-1)} \\ \mathbf{0} \end{bmatrix} + \begin{bmatrix} \mathbf{0} \\ {}^{t+\Delta t}\Delta_C^{(i-1)} \end{bmatrix} \quad (14)$$

where,

- ${}^{t+\Delta t} \underline{\mathbf{K}}_C^{(i-1)}$ is the cable structure regular stiffness matrix, after $(i-1)$ iterations, associated to finite element incremental displacements $\Delta U^{(i)}$;
- ${}^{t+\Delta t} \underline{\mathbf{K}}_\lambda^{(i-1)} = [-\mathbf{n}_j^S]$ is the cable structure stiffness matrix contribution to coupling of regular finite element incremental displacements and Lagrange multiplier degrees-of-freedom $\lambda^{(i)}$;
- ${}^{t+\Delta t} \mathbf{R}$ is the external forcing vector;
- ${}^{t+\Delta t} \mathbf{F}^{(i-1)}$ is the internal forcing vector, after $(i-1)$ iterations;
- ${}^{t+\Delta t} \Delta_C^{(i-1)} = [(\mathbf{n}_j^S)^T {}^{t+\Delta t} \Delta_K^{(i-1)}]$ is the material superposition measured in the seabottom normal direction, associated to each contact node K, after $(i-1)$ iterations.

3. Numerical Analysis of a Flexible Line

When considering a long flexible line, the catenary configuration can lead to very high axial loads, especially at the floating vessel connection and at the zone of contact between the flexible line and the sea bottom, more specifically at the TDP - "touch down point" (Lustosa, 2000). To minimize these effects submerged buoys are generally added to the line to allow it for alternative configurations, unloading the line, as shown in Fig. 2. Numerical analysis results for this type of arrangement configuration was presented by Mourelle, 1993, using the same geometric and physical parameters shown in Larsen, 1992, that reports the numerical results finished by various research institutions, using ten different commercial programs: Riser, Flexcom - 3D, Fenris, Flexan - F, Seapipe, Orcaflex, Aqwaflex, Riflex, Mobdex and Reflex. In this example numerical, results obtained from the present study are compared to the ones reported by Mourelle, 1993, by Larsen, 1992, and in analysis results performed with ANFLEX-Finite Element Program for the Analysis of Flexible Risers software. In fig 2, a flexible line typical static configuration is presented. It may be noticed that along the CFB line segment, 31 buoys - 1.0 m in length, 2.0 m. apart - are installed. Physical and geometric cable characteristics used in the numerical analyses are presented in Table 1(a).

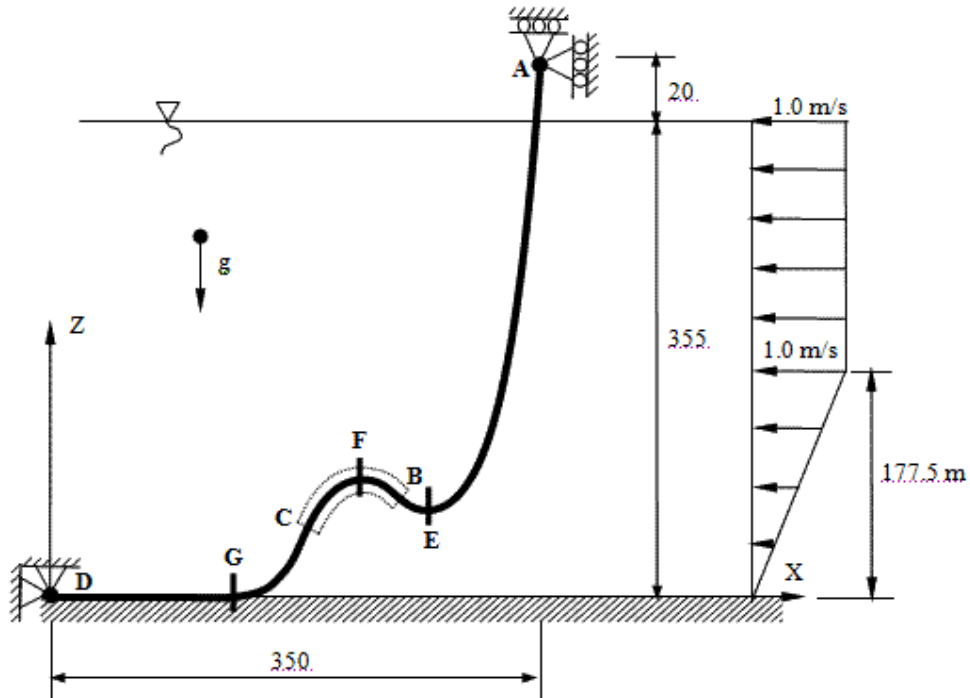


Figure 2.- Geometric Configuration for the "Lazy Wave" Riser Considered

In the finite element model representation and analysis the following line characteristics had been considered:

- (a) analysis fluid loading on the line results from normal and tangential force components, obtained from Morrison's formula ;
- (b) cable flexural rigidity is modified by the submerged buoys added to the line ;

(c) wave effects are not considered in this work. Thus, in the numerical models the following loadings are included: gravitational, buoyancy, current and due to prescribed motion at point A of the line. In Table 1(b) the current profile characteristics considered is presented;

(d) phase and amplitude parameters for the platform prescribed motion at line point A, are the same ones furnished in Mourelle, 1993 and are shown in Table 1(b);

(e) friction effects between the riser and the seabottom are not considered.

Table 1 - Physical Parameters Used in the Model Analysis
(a) Flexible Line

| | |
|--|------------------------------|
| Riser Sections (200m + 360m): | |
| Axial Stiffness (EA) | 10000 KN |
| Bending Stiffness (EI) | 6.57 KN m ² |
| Torsion Stiffness (GJ) | 1000 KN m ² / rad |
| Dry weight, including internal fluid | 0.87309 KN / m |
| External Diameter | 0.2154 m |
| Riser Section with Buoys (91m): | |
| Axial and Torsional Stiffness | Unchanged |
| Bending Stiffness (EI) | 100 KN m ² |
| Dry weight, including internal fluid | 3.453 KN / m |
| Hydrodynamic Coefficients (both sections) | |
| Inertia Force Coefficient (CM) | 2.0 |
| Normal Drag Coefficient (CDn) | 1.0 |
| Tangential Drag Coefficient (CDt) | 0.05 |

(b) Current and Prescribed Motion Characteristics

| | |
|------------------------------|--------------------------|
| Current Profile : | |
| Bottom 0.0 m | 0.0 m/s |
| Mid-waterdepth | 1.0 m/s |
| Surface | 1.0 m/s |
| X-direction Motion : | |
| Period (T _x) | 12 s |
| Amplitude (X ₀) | 4.0 m |
| Phase (φ _x) | 20.43° |
| Z-direction Motion : | |
| Period (T _z) | 12 s |
| Amplitude (Z ₀) | 6.0 m |
| Phase (φ _z) | -110.43° |
| Sea water Specific Weight | 10.055 KN/m ³ |

The 651m long riser was modeled using 135 elements in 3 segments: in the first 200m twenty equally spaced elements was used; in the second, a 91m long segment, ninety-one elements were used representing the floats, and; the third, a with 360 m long segment, was modeled by 24 elements. The line initial configuration results from static equilibrium, considering gravity and buoyancy loads only, which are used as initial condition for the dynamic analysis. As in Larsen, 1992, loadings and obtained coordinates of some points along the line are used to evaluate the finite element models, at (see Fig. 2): the most far right node (point A), the most far left node, on the sea bottom (point D), the highest point of the line floating segment (point F) and the contact point with sea bottom "touch down point" (point G). At location points A and D the traction loads are reported and, at location points G the horizontal coordinate position is presented and at F both x-z coordinates and curvature of the riser are reported. These comparisons are presented in the Table 2. It may be noticed that except for one result for the traction loading at point D, the numerical results are in very good agreement.

In Table 3 a similar comparison is presented for the static analysis results including the effects of the marine current. As in Table 2 a good result agreement was obtained except for the traction force evaluated at point D, in one of the analysis. The riser final static configuration is shown in Fig. 3, comparing present study solutions with the results from ANFLEX program. To illustrate the numerical procedure used riser intermediate configurations are also presented, starting from the initial catenary shape – closed form solution - obtained from gravitational and buoyancy loads only. Convergence to the static equilibrium was obtained after 49 numerical iterations what is, naturally, much higher than in

analyses where no contact effects occur. To minimize this computational effort, current and buoyancy loads are gradually applied, in a smaller time steps. Numerical tests have shown that this strategy results in a smaller number of

Table 2 – Comparison from Different Software Numerical Results – Static Analysis with No Current

| Reference Analyses | Traction at Point A (KN) | Traction at Point D (KN) | Point G x-coord (m) | Point F | | |
|--------------------|--------------------------|--------------------------|---------------------|--------------------|------------------|--------------------------|
| | | | | x (mm) | z (mm) | Curvature $10^{-2}(1/m)$ |
| (Larsen, 1992) | 176.8 ± 3.26 | 19.0 ± 20.9 | 140.0 ± 7.42 | 225.1 ± 2.26 | 79.34 ± 2.01 | 3.57 ± 1.12 |
| (Mourelle, 1993) | 177.8 (0.75 %) | 3.6 (-70.3 %) | 145.0 (0.3 %) | 224.0 (-0.05 %) | 81.0 (-0.4 %) | 3.73 (-2.6 %) |
| ANFLEX | 176.10 (-0.2 %) | 12.17 (0.6 %) | 140.56 (-2.8 %) | 224.67 (0.25 %) | 81.97 (0.8 %) | 3.66 (-4.4 %) |
| Present Study | 176.47 | 12.1 | 144.62 | 224.11 | 81.32 | 3.83 |

iterations required in the analysis. Apart from these difficulties, a good agreement was observed for the final configurations obtained from both analysis comparisons. Note that these results occur despite friction conditions not being included in the present study and in ANFLEX analysis indicating that effects of longitudinal friction at the contact region can be neglected, at least for the case study analysis considered. The obtained riser configuration, with zero velocity, is used as initial conditions in the dynamic analysis discussed in the following.

Table 3– Numerical Comparison from Different Numerical Software Results – Static Analysis with Current Included

| Reference Analyses | Traction at Point A (KN) | Traction at Point D (KN) | Point G x-coord (m) | Point F | | |
|--------------------|--------------------------|--------------------------|---------------------|--------------------|--------------------|--------------------------|
| | | | | x (mm) | z (mm) | Curvature $10^{-2}(1/m)$ |
| (Larsen, 1992) | 173.7 ± 3.69 | 16.0 ± 19.8 | 142.0 ± 6.10 | 209.2 ± 3.08 | 88.24 ± 1.64 | 4.985 ± 2.46 |
| (Mourelle, 1993) | 176.1 (1.64 %) | 2.3 (-71.1 %) | 145.0 (0.3 %) | 211.2 (-0.56 %) | 89.5 (0.09 %) | 5.13 (-5 %) |
| ANFLEX | 174.33 (0.62 %) | 7.75 (-2.76 %) | 140.67 (-2.7 %) | 212.76 (0.17 %) | 89.17 (-0.28 %) | 6.97 (29.3 %) |
| Present Study | 173.25 | 7.97 | 144.56 | 212.39 | 89.42 | 5.39 |

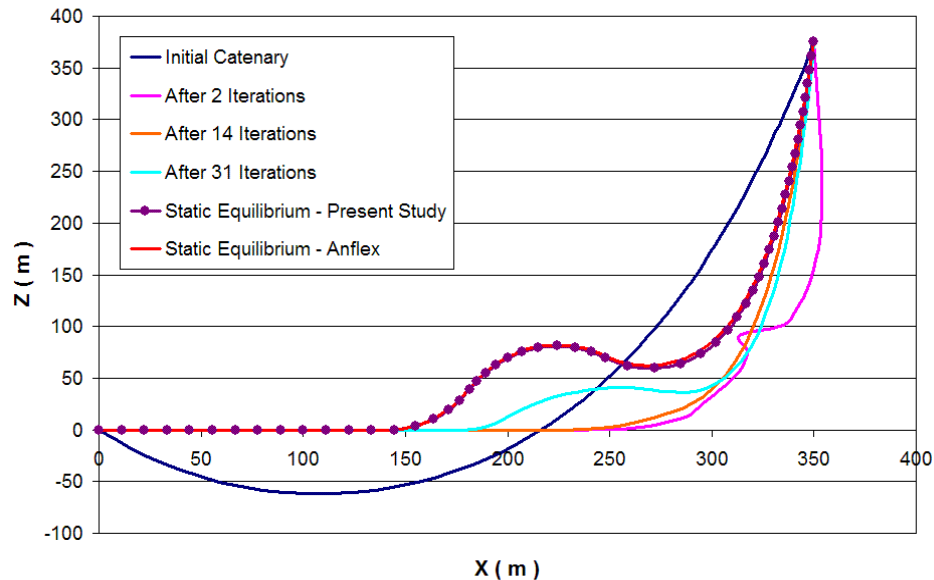


Figure 3 – Initial, Intermediates and Final Riser Configurations in the Static Analysis

Considering the dynamic analysis of the flexible riser, additional prescribed motions at point A are added to the model, in the form $X_A(t) = 350 + X_0 \cos(2\pi t / T_x + \phi_x)$ and $Z_A(t) = 375 + Z_0 \cos(2\pi t / T_z + \phi_z)$, where the defining parameters are shown in Table 1(b). The numerical analysis employed a time step increment of 0.05 s, as suggested by the carried through numerical tests in (Mourelle, 1993), for an analysis time span of 30 second. Temporal integration

was performed using Newmark time integration procedure in its implicit form for integration parameters $\alpha = 0.5625$, $\delta = 1$ (corresponding to the limit values for the stability), and the structural Rayleigh damping coefficient $\beta d = 0.005$. Overall maximum and minimum numerically obtained traction force values at attachment point A, are presented in Table 4, and compared with the corresponding results with ANFLEX program. A good agreement for these results is observed.

Figure 4 depicts successive configurations from the riser in dynamic analysis, at times 18-21-24-27 and 30s. Following recommended procedures in (Lustosa, 2000; Mourelle, 1993), time transition functions for the prescribed motion had been used at point A, preventing numerical difficulties in dealing with impact loadings. In these figures detailed results near the riser connecting point A and TDP are also included, because the figure scale shows relative small dynamic motions, within the static solution configuration. Although small, position results from both numerical model analysis compared well. In Figure 4 traction force values, along the cable's length, obtained from the present formulation are shown and compared to ANFLEX model solution, at the same times considered previously. In these graphs the first peak for the traction force occurs at the beginning of the submerged buoys – point C, in Figure 2 – and decays until end point B, when it gets raise again until the extreme point A. These results show the importance of the appropriate use and location for the buoys along the flexible line.

Table 4 – Traction Force Maximum Values at Point A

| Carried Through Analyses | Traction Forces at Point A (kN) Current / Prescribed Motion | | |
|--------------------------|--|----------------|--------------------------------|
| | T_{Max} | T_{Min} | $\Delta T = T_{Max} - T_{Min}$ |
| ANFLEX | 226.96 (-0.54%) | 116.43 (-3.7%) | 110.54 (3 %) |
| Present Study | 228.20 | 120.91 | 107.29 |

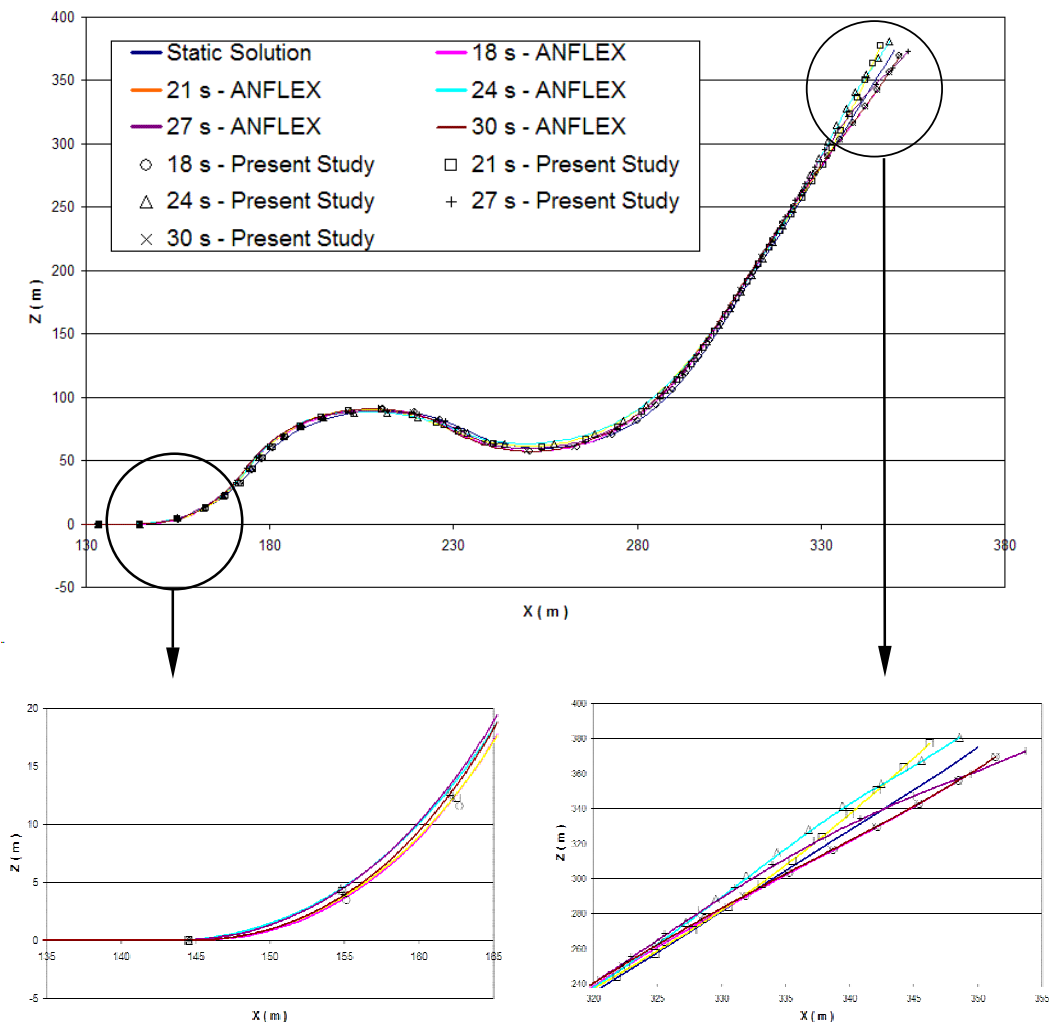


Figure 4 - Cable Configurations in Dynamic Analysis

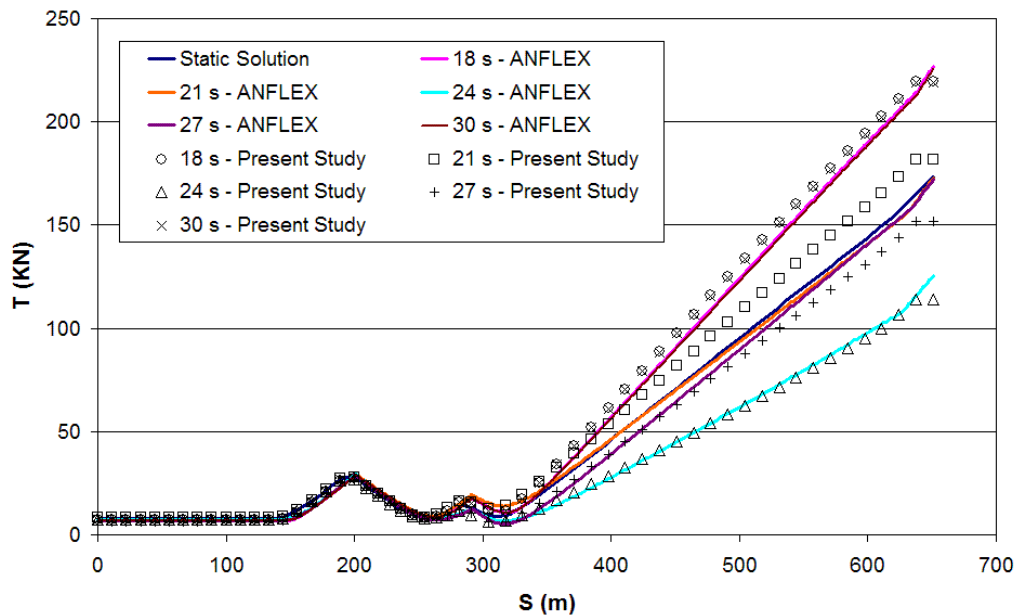


Figure 5 – Numerical Solutions for Traction Forces Along the Riser

4. Conclusions

An algorithm for the dynamic analysis of two-dimension risers, including contact with the seabottom, has been presented. The solution procedure uses the formulation for large displacement Hermitian beam elements to represent the cable dynamics and Lagrange multiplier technique to incrementally impose the riser deformation constraints along the contact with seabed, assume flat and rigid. The traction forces at the contact are calculated from nodal point forces with no friction effects. The solution results obtained using the algorithm in a sample “lazy wave” riser configuration has been presented to demonstrate some of the solution procedure features.

In this paper we have concentrated on presenting the theory used and indicating in one application its most important characteristics. However other testing results have been performed with the formulation have been most encouraging and because some aspects of paramount importance are not yet evaluated and deserve further studies (Andrews, 2004), such as:

1. The effects of an irregular seabed configuration on the riser dynamics;
2. Effective modeling of constraints including friction conditions, specially suitable for three-dimension analysis;
3. An adaptive finite element model to adequately represent the seabottom flexibility, using one-dimension formulation;
4. Further studies on the implementation of numeric damping to avoid high-frequency vibrations in the riser dynamic responses, aiming for fast solution convergences.

These studies would provide yield further insight into the solution procedure and provide the basis for improvements in the solution method.

3. Acknowledgements

We are grateful for the financial support provided to A. T. Andrews by ANP (Agencia Nacional de Petroleo), for his MSc. studies at PUC-Rio.

4. References

- Almeida, C.A.,Lustosa, E.M.,1999,“Three-Dimension Finite Element Modeling for The Representation of Marine Cable Dynamics”, Dynamic Problems in Mechanics and Mechatronics Proc. (EuroDiname’99), July, 11-16.
- Andrews, A.T., 2004,“Analise Bidimensional da Dinâmica de Linhas Flexíveis Incluindo o Contato com o Fundo Marinho”, PUC-Rio, MSc. Thesis(in portuguese)
- Bathe, K.J., 1996, Finite Element Procedures, Prentice-Hall.
- Bathe, K.J. and Chaudhary, A.,1985 ”A Solution Method for Planar and Axisymmetric Contact Problems”, Int. J. for Num. Meth. In Engn,v.21,pp.65-88.
- Ghadimi, R.,1988,“A Simple and Efficient Algorithm for the Static and Dynamic Analysis of Flexible Marine Risers”,

- Computers and Structures, vol.29, no.4, pp.541-555.
- Larsen, C.M., 1992, "Flexible Riser Analysis – Comparison of Results from Computer Programs", Journal of Marine Structures, v. 5, pp. 103-119.
- Lustosa, E.M., 2000, "Dinâmica de Linhas Marítimas pelo Método dos Elementos Fintos", PUC-Rio, MSs Thesis (in portuguese).
- McNamara, J.F. and Hibbit, H.D., 1986, "Numerical Analysis of Flexible Pipes and Risers in Offshore Applications", Proc. 1st. Offshore Mechanics and Arctic Engineering Specialty Symp. on Offshore and Arctic Frontiers, New Orleans.
- Mourelle, M.M., 1993, "Análise Dinâmica de Sistemas Estruturais Constituídos por Linhas Marítimas", COPPE/UFRJ, DSc Thesis (in portuguese).
- O'Brien, P.J.; McNamara, J.F., 1989, "Significant Characteristics of Three-dimension Flexible Riser Analysis", Engineering Structures, v. 11, pp. 223-233.
- Oden, J.T., 1981, "Exterior Penalty Methods for Contact Problems", in Nonlinear Finite Element Analysis in Structural Mechanics, (W. Wunderlich et al., Eds) Springer-Verlag.
- Ractliffe, A.T., 1984, "Dynamic Response of Flexible Catenary Risers", International Symposium on Developments in Floating Production Systems.
- Yau, A.O., 1982, "Solution of 2-D Contact Problems Using a Variational Formulation with Lagrange Multipliers", M.I.T., S.M. thesis, Department of Mechanical Engineering.

5. Responsibility notice

The authors are the only responsible for the printed material included in this paper.